



# Automated 3D Analysis of Clinical Magnetic Resonance Images Demonstrates Significant Reductions in Cam Morphology Following Arthroscopic Intervention in Contrast to Physiotherapy

Jessica M. Bugeja, B.E., Ying Xia, Ph.D., Shekhar S. Chandra, Ph.D.,  
 Nicholas J. Murphy, M.B.B.S., B.A., B.Med.Sc.,  
 Jillian Eyles, Ph.D., B.App.Sc. (Physiotherapy),  
 Libby Spiers, B.App.Sc. (Physiotherapy), Stuart Crozier, Ph.D.,  
 David J. Hunter, M.B.B.S. (Hons), M.Sc. (Clin Epi), M. Sp. Med., Ph.D., F.R.A.C.P.  
 (Rheum), Jurgen Fripp, Ph.D., and Craig Engstrom, Ph.D.

**Purpose:** To obtain automated measurements of cam volume, surface area, and height from baseline (preintervention) and 12-month magnetic resonance (MR) images acquired from male and female patients allocated to physiotherapy (PT) or arthroscopic surgery (AS) management for femoroacetabular impingement (FAI) in the Australian FASHIoN trial. **Methods:** An automated segmentation pipeline (CamMorph) was used to obtain cam morphology data from three-dimensional (3D) MR hip examinations in FAI patients classified with mild, moderate, or major cam volumes. Pairwise comparisons between baseline and 12-month cam volume, surface area, and height data were performed within the PT and AS patient groups using paired *t*-tests or Wilcoxon signed-rank tests. **Results:** A total of 43 patients were included with 15 PT patients (9 males, 6 females) and 28 AS patients (18 males, 10 females) for premanagement and post-management cam morphology assessments. Within the PT male and female patient groups, there were no significant differences between baseline and 12-month mean cam volume (male: 1269 vs 1288 mm<sup>3</sup>, *t*[16] = -0.39; female: 545 vs 550 mm<sup>3</sup>, *t*[10] = -0.78), surface area (male: 1525 vs 1491 mm<sup>2</sup>, *t*[16] = 0.92; female: 885 vs 925 mm<sup>2</sup>, *t*[10] = -0.78), maximum height (male: 4.36 vs 4.32 mm, *t*[16] = 0.34; female: 3.05 vs 2.96 mm, *t*[10] = 1.05) and average height (male: 2.18 vs 2.18 mm, *t*[16] = 0.22; female: 1.4 vs 1.43 mm, *t*[10] = -0.38). In contrast, within the AS male and female patient groups, there were significant differences between baseline and 12-month cam volume (male: 1343 vs 718 mm<sup>3</sup>, *W* = 0.0; female: 499 vs 240 mm<sup>3</sup>, *t*[18] = 2.89), surface area (male: 1520 vs 1031 mm<sup>2</sup>, *t*(34) = 6.48; female: 782 vs 483 mm<sup>2</sup>, *t*(18) = 3.02), maximum-height (male: 4.3 vs 3.42 mm, *W* = 13.5; female: 2.85 vs 2.24 mm, *t*(18) = 3.04) and average height (male: 2.17 vs 1.52 mm, *W* = 3.0; female: 1.4 vs 0.94 mm, *W* = 3.0). In AS patients, 3D bone models provided good visualization of cam bone mass removal postostectomy. **Conclusions:** Automated measurement of cam morphology from baseline (pre-intervention) and 12-month MR images demonstrated that the cam volume, surface area, maximum-height, and average height were significantly smaller in AS patients following ostectomy, whereas there were no significant differences in these cam measures in PT patients from the Australian FASHIoN study. **Level of Evidence:** Level II, cohort study.

From the School of Information Technology and Electrical Engineering, The University of Queensland, Australia (J.M.B., S.S.C., S.C.); Australian e-Health Research Centre, CSIRO Health and Biosecurity, Australia (J.M.B., Y.X., J.F.); Kolling Institute of Medical Research, Institute of Bone and Joint Research, University of Sydney, Australia (N.J.M., J.E., D.J.H.); Department of Orthopaedic Surgery, John Hunter Hospital, Newcastle, Australia (N.J.M.); Department of Rheumatology, Royal North Shore Hospital, St. Leonards, Australia (J.E., D.J.H.); Centre for Health, Exercise and Sports Medicine, Department of Physiotherapy, University of Melbourne, Melbourne, Australia (L.S.); and School of Human Movement Studies, The University of Queensland, Australia (C.E.)

The authors report the following potential conflicts of interest or sources of funding: S.S.C. reports grants from the National Health and Medical Research Council, during the conduct of this study. S.C. reports grants from National Health and Medical Research Council, during the conduct of the study; and is the director of Magnetica Pty Ltd, outside the submitted work. D.J.H. reports

personal fees from Pfizer, Lilly, TLCBio, Novartis, Tissuegene, and Biobone, outside the submitted work. J.F. reports grants from National Health and Medical Research Council, during the conduct of the study. C.E. reports grants from National Health and Medical Research Council, during the conduct of the study. Full ICMJE author disclosure forms are available for this article online, as [Supplemental Material](#).

Received December 27, 2021; accepted April 19, 2022.

Address correspondence to Jessica M. Bugeja, B.E., School of Information Technology and Electrical Engineering, The University of Queensland, St. Lucia, QLD, 4072, Australia. E-mail: [jessica.bugeja@uq.net.au](mailto:jessica.bugeja@uq.net.au)

© 2022 THE AUTHORS. Published by Elsevier Inc. on behalf of the Arthroscopy Association of North America. This is an open access article under the CC BY-NC-ND license (<http://creativecommons.org/licenses/by-nc-nd/4.0/>). 2666-061X/211799

<https://doi.org/10.1016/j.asmr.2022.04.020>

## Introduction

Clinically, cam-type femoroacetabular impingement (FAI) syndrome is a symptomatic, activity-related condition attributed to repetitive pathognomonic contact between the proximal femur and acetabulum during hip flexion and internal rotation.<sup>1,2</sup> Cam morphology is characterized by an aspherical femoral head due to an osseous convexity located in the anterior and/or the antero-superior femoral head-neck region.<sup>3</sup> Recently, Bugeja et al.<sup>4</sup> described CamMorph, an automated segmentation and analysis framework integrating U-net+focused shape modeling (FSM) approaches, to calculate cam volume, surface area, and height from three-dimensional (3D) magnetic resonance (MR) images of the hip from FAI patients in the Australian FASHIoN study.<sup>5</sup> In automated analyses of baseline MR images from these patients, the cam volume, surface area, maximum height and average height were all significantly greater in males compared to females<sup>4</sup> in line with previous findings from semi-automated analyses of cam morphology in patients with FAI.<sup>6,7</sup>

The purpose of the present study was to obtain automated measurements of cam volume, surface area, and height from baseline (preintervention), and 12-month MR images acquired from male and female patients allocated to physiotherapy (PT) or arthroscopic surgery (AS) management for FAI in the Australian FASHIoN trial. It was hypothesized that there would be no significant difference between the baseline and 12-month cam volume, surface area, maximum height, and average height for the PT-managed patients. It was hypothesized that the 12-month cam volume, surface area, maximum height, and average height would be significantly smaller than the baseline values for the AS-managed patients.

## Methods

### Study Population and MR Image Acquisition

The present study analyzed MR images of the hip joint from FAI patients allocated to either PT or AS management in the Australian FASHIoN study,<sup>5</sup> a multicenter randomized controlled trial assessing cartilage.<sup>8</sup> All patients recruited for the Australian FASHIoN trial had hip pain, radiographic signs of cam and/or pincer morphology and had a surgical opinion that they would benefit from arthroscopic hip surgery. For further information on patient inclusion and exclusion criteria, refer to Murphy et al.'s article.<sup>5</sup>

In the present study, patients with a cam volume classified (as per Bugeja et al.<sup>4</sup>) as mild, moderate, or major determined from baseline MR examinations, who had both baseline and 12-month MR examinations with appropriate coverage of the femoral head-neck region of interest (ROI) and images free of

major contrast or artefact distortions were included for initial analysis. In the Australian FASHIoN trial, surgeons performed arthroscopic procedures, according to their usual practice and positioning (supine or lateral) protocols. The MR images used in the present study were acquired with a 3D T2-weighted true fast imaging with steady-state precession (true-FISP) sequence (repetition time: 10.2 ms, echo time: 4.3 ms, weighted average image spacing (image spacing varied in this multisite study):  $0.644 \times 0.644 \times 0.668$  mm, field of view:  $16 \times 16$  cm, matrix size:  $256 \times 256$ ).

### Manual Segmentation of Proximal Femur Volume

Manual segmentations of the proximal femur were performed by J.M.B., under expert guidance from C.E., on the baseline and 12-month MR examinations in a random sub-sample of PT ( $N = 22$ ) and AS patients ( $N = 22$ ) from the FASHIoN dataset to evaluate the fit of the 3D U-net+FSM segmentations used in the automated CamMorph pipeline. The agreement between the manual and automated 3D segmentations of the proximal femur (femoral head, neck, and proximal shaft) was assessed using the Dice similarity index (DSI)<sup>9</sup> for volume overlap (1 representing perfect overlap and 0 representing no overlap) and surface distance differences (mm) based on the 95% Hausdorff distance (HD)<sup>10</sup> and average surface distance (ASD).<sup>11</sup> The manual segmentations, in combination with the 3D FSM and focused cam region in the present study (refer to Part A of the [Supplemental Fig S1](#)), were also used for qualitative topological evaluation of ostectomy sites and cam morphology characteristics of the AS and PT patients, respectively.

### Cam Volume, Surface Area, and Height Measurements

In the current study, the CamMorph pipeline<sup>4</sup> was modified for the analysis of the 12-month MR images from the PT and AS patients. This modification involved an initial coregistering of the femur surfaces fitted to a baseline and 12-month MR image using a bounded iterative closest points algorithm (VTK implementation<sup>12</sup>). This algorithm focused on the femoral head-neck ROI to facilitate the registration fitting of the cam morphology region in baseline and 12-month MR bone models.<sup>13</sup> The ROI was initialized using Xia et al.'s<sup>13</sup> method. After this model registration, the FSM "healthy" bone relaxation in the femoral head-neck ROI of the baseline femur model was completed as per Bugeja et al.'s study.<sup>4</sup> Following the relaxation step, the signed distance map between the healthy (relaxed baseline model) and cam-affected femur surfaces (baseline and 12-month) was completed to identify cam morphology within the contoured cam region (refer to Part A of [Supplemental Fig S1](#) for cam ROI visualization). Voxels within the

cam morphology region with a distance of more than 0 mm were included as part of the cam bone mass for volume, surface area, and height measurements.

### Statistical Analyses

Pairwise comparisons between baseline and 12-month cam volume, surface area, maximum-height, and average-height data were performed within the PT and AS patient groups using paired *t*-tests or Wilcoxon signed-rank tests. These analyses were conducted on male and female patients separately on the basis of previous reports of sexual dimorphism in cam morphology,<sup>4,6,7</sup> which, in the present study, was confirmed in a separate cross-sectional analysis of the male and female patient data (Refer to Part B of the [Supplemental Material](#)). Prior to performing the pairwise comparisons between baseline and 12-month cam morphology data, the Shapiro-Wilk test was applied to check the normality of the data, and Wilcoxon signed-rank tests were used if the data did not have a normal distribution. For the *t*-test analyses, Levene's method was used to assess homogeneity of variances, and Welch's test was applied if samples did not have equal variances. Statistical significance was set a priori at  $P < .05$ , and all statistical analyses were calculated using a python package, SciPy.<sup>14</sup>

## Results

From an available pool of 51 patients, 2 patients did not have their final treatment recorded, and 6 AS patients did not undergo femoral ostectomy procedures and, thus, were excluded from the present analyses. For the final cam morphology analysis, MR data were included from 43/51 (84%) of the patients, consisting of 15 PT patients (9 males, 6 females, aged 16 to 44 years, body mass index (BMI) 20 to 27 kg/m<sup>2</sup>) and 28 AS (with femoral ostectomy) patients (18 males, 10 females, aged 16 to 63 years, BMI 19 to 33 kg/m<sup>2</sup>).

### Proximal Femoral Bone Segmentation

[Figure 1](#) shows boxplots for the DSI ([Fig 1A](#)), 95% HD ([Fig 1B](#)) and ASD ([Fig 1C](#)) values between the manual and automated segmentations of the proximal femur volume. Overall, the mean DSI values showed excellent agreement between the manual and automated segmentations of the baseline ( $0.965 \pm 0.006$ ) and 12-month ( $0.964 \pm 0.007$ ) proximal femur volumes. The mean 95% HD values between the manual and automated segmentations of the proximal femur for the baseline and 12-month comparisons were  $1.98 \pm 0.71$  mm and  $2.15 \pm 0.87$  mm, respectively. The mean ASD values for the proximal femur segmentations for the baseline and 12-month comparisons were  $0.51 \pm 0.13$  mm and  $0.53 \pm 0.16$  mm, respectively.

In [Fig 1](#), three outlier cases in the boxplots are shown with accompanying MR images and automated

segmentations. The coronal MR images show all three cases have a limited field of view of the proximal femur with little or no coverage of the greater trochanter, as well as varying imaging quality in terms of artefacts and irregular signal intensity characteristics, which likely affected the FSM fitting and contributed to the reduced segmentation performance in these individual cases.

[Figure 2](#) shows 3D femoral bone models for visualization of the mean and standard deviation 95% HD values between the manual and automated segmentations of the proximal femur for the PT and AS patients from baseline and 12-month analyses. Across the anterior and antero-superior regions of the femoral head-neck region, the commonest site for cam formations in symptomatic FAI patients, the mean 95% HD values are below 0.67 mm in both the baseline and 12-month analyses. This robust fitting of the FSM in these primary areas of clinical interest for both the baseline and 12-month segmentations, the latter involving bone segmentation performed following invasive ostectomy procedures in AS patients, demonstrates the excellent performance of this modeling approach, which underpins the CamMorph pipeline for automated calculation of cam morphology.

### Cam Morphology in PT Patients

Mean and standard deviation data for baseline and 12-month cam volume, surface area, maximum height, and average height for PT male and female patients are provided in [Table 1](#). The pairwise analysis of the data within the male PT patients showed no significant difference between baseline and 12-month mean cam volume ( $t[16] = -0.39, P = .710, \text{Fig 3A}$ ), surface area ( $t[16] = 0.92, P = .386; \text{Fig 3B}$ ), maximum height ( $t[16] = 0.34, P = .744, \text{Fig 3C}$ ) or average-height ( $t[16] = 0.22, P = .831; \text{Fig 3D}$ ). Similarly, within the female PT patients, there was no significant difference between the baseline and 12-month mean cam volume ( $t[10] = -0.12, P = .911, \text{Fig 3A}$ ), surface area ( $t[10] = -0.78, P = .470; \text{Fig 3B}$ ), maximum height ( $t[10] = 1.05, P = .343; \text{Fig 3C}$ ) or average height ( $t[10] = -0.38; P = .718, \text{Fig 3D}$ ).

[Figure 4](#) shows 3D models of the proximal femur generated in SMILI<sup>15</sup> to visualize the baseline and 12-month cam profiles in individual PT male and female patients classified as having a baseline mild, moderate, or major cam volume, as calculated from the CamMorph pipeline. Topologically, there is very little (or no) observable difference in the cam location and profile in the femoral head-neck ROI between the baseline and 12-month comparisons for each of the individual male and female patients within each of the cam volume categories. The consistency between the baseline and 12-month visualizations of the cam topology in these individual PT male and female patients indicates that the cam bone mass has remained

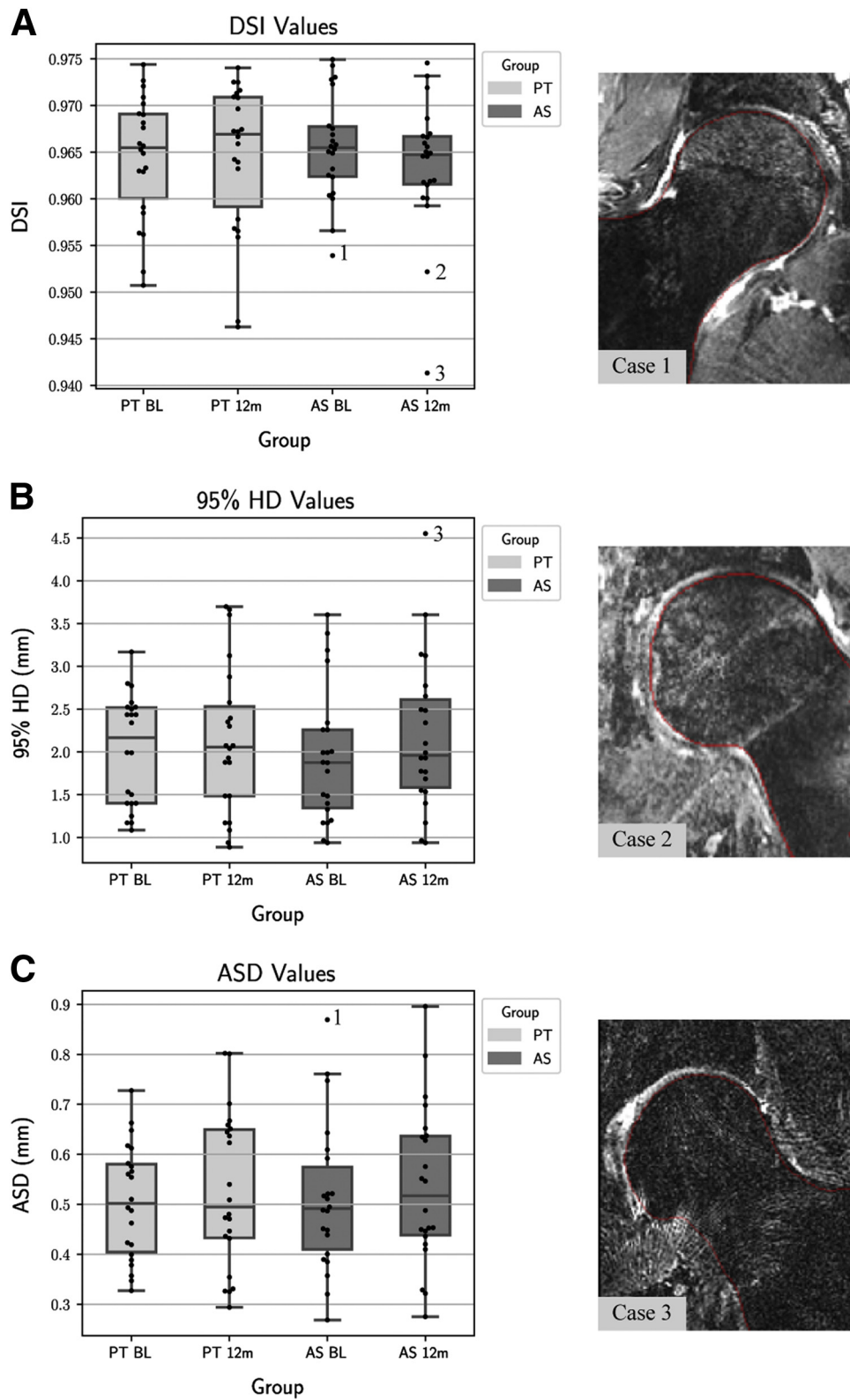


**Fig 1.** Boxplots of the DSI (A), 95% HD (B) and ASD (C) values between the manual and automated segmentations of the proximal femur (the boxplot centerline marks the median value). The included coronal MR images with an automated segmentation contour overlaid are for 3 outlier cases with image contrast and field of view insufficiencies. AS, arthroscopic surgery; ASD, average surface distance; BL, baseline; DSI, Dice similarity index; HD, Hausdorff distance; PT, physiotherapy management; 12m, 12-month.

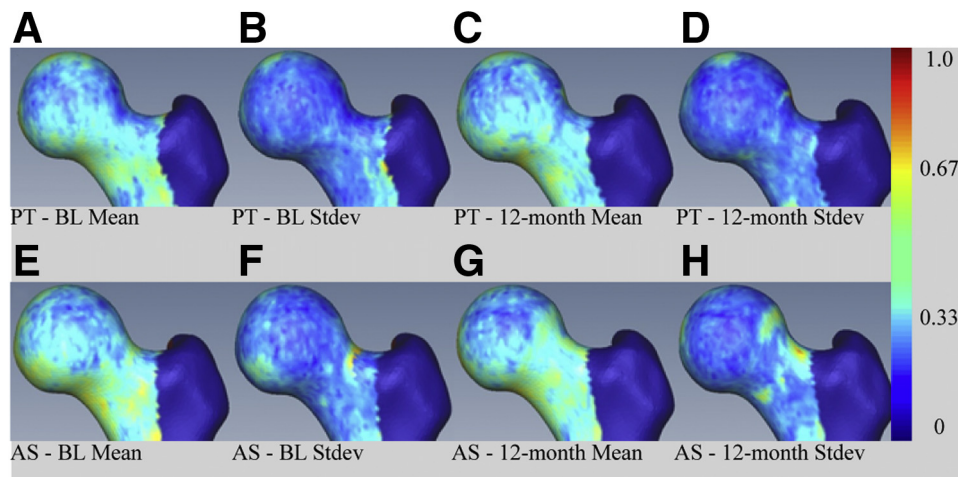


**Fig 2.** Visualization of the mean 95% Hausdorff distance between the fitted FSM and the manual segmentations of the proximal femur for the PT (A-D) and AS management groups (E-H) for baseline (columns 1 and 2) and 12-month segmentations (columns 3 and 4). The mean (columns 1 and 3) and standard deviation (columns 2 and 4) 95% Hausdorff distance scalars are displayed. Note that the greater trochanter region, which is not of primary clinical interest in the current study for cam bone mass assessment, has been “masked” to exclude it from the above visualization. The scalar bar was capped at 1 mm to help with the visualization of differences present in the femoral head-neck region rather than those differences around the greater trochanter. AS, arthroscopic treatment group; BL, baseline; FSM, focused shape model; PT, physiotherapy management group; stdev, standard deviation.

very stable during the PT intervention period of the Australian FASHIoN study.

### Cam Morphology in AS Patients

Mean and standard deviation data for baseline and 12-month cam volume, surface area, maximum height, and average height are provided in [Table 2](#) for the AS male and female patients. The pairwise analysis of the cam morphology data within the male AS patients showed, that in comparison with the baseline (prearthroscopy) data, the 12-month data demonstrated a significantly reduced median cam volume ( $W = 0.0$ ,  $P < .001$ ; [Fig 5A](#)), mean surface area ( $t[34] = 6.48$ ,  $P < .001$ ; [Fig 5B](#)), median maximum height ( $W = 13.5$ ,  $P = .002$ ; [Fig 5C](#)) and median average height ( $W = 3.0$ ,  $P < .001$ ; [Fig 5D](#)). Similarly, pairwise analyses of cam morphology data within the female AS patients revealed, that in comparison with baseline data, the 12-month data demonstrated a significantly reduced mean cam volume ( $t[18] = 2.89$ ,  $P = .018$ ; [Fig 5A](#)), surface area ( $t[18] = 3.02$ ,  $P = .015$ ; [Fig 5B](#)), maximum-height ( $t[18] = 3.04$ ,  $P = .014$ ; [Fig 5C](#)), and median average height ( $W = 3.0$ ,  $P = 0.012$ ; [Fig 5D](#)).

The median and interquartile range of the resected cam volume, surface area, maximum height, and average height data are provided in [Table 3](#) for the AS male and female patients.

[Figure 6](#) shows 3D models of the proximal femur for the baseline and 12-month cam profiles in individual male and female AS patients classified as originally having a baseline mild, moderate, or major cam

volume. The 3D models clearly show cam bone mass reduction between the baseline (prearthroscopy) and 12-month profiles of the head-neck ROI for each of the individual patients within the different cam volume categories. Inspection of the baseline and 12-month cam profiles in the 3D models of the proximal femur in all the AS patients indicated that, in the majority of cases, the greatest bone removal occurred in the anterior and antero-superior femoral head-neck region with less bone removal evident in other locations such as the antero-inferior region.

### Discussion

In male and female patients with FAI, automated measurement of cam morphology from baseline and 12-month MR images demonstrated that the cam volume, surface area, maximum height and average height were significantly reduced following surgery in AS-managed patients. Conversely, there were no significant differences in these cam morphology measures in PT patients following the management protocol used in the Australian FASHIoN trial. Following osteotomy, reductions in cam bone mass between the preoperative and postoperative MR images in individual patients could be clearly visualized in 3D bone models of the proximal femur for AS patients with baseline mild, moderate, and major cam volumes.

### Proximal Femur Segmentation

The automated 3D U-net+FSM segmentations of the proximal femur volume, which underpin the cam

**Table 1.** Mean and Standard Deviation Data for Baseline and 12-Month Cam Volume, Surface Area, Maximum-Height and Average-Height in the Male and Female PT Patients

	Male ( <i>n</i> = 9)		Female ( <i>n</i> = 6)	
	Baseline	12-Month	Baseline	12-Month
Volume (mm <sup>3</sup> )	1269.19 ± 301.28	1287.73 ± 381.24	544.69 ± 204.95	550.06 ± 128.22
Surface area (mm <sup>2</sup> )	1524.56 ± 160.14	1490.56 ± 200.80	885.34 ± 161.95	925.22 ± 108.21
Maximum height (mm)	4.36 ± 1.46	4.32 ± 1.42	3.05 ± 0.69	2.96 ± 0.56
Average height (mm)	2.18 ± 0.69	2.18 ± 0.64	1.40 ± 0.36	1.43 ± 0.29

PT, physiotherapy.

morphology measures from the CamMorph pipeline, demonstrated excellent agreement with the manual segmentations having very high DSI values comparable to previous MR validation studies.<sup>16-20</sup> For the current clinical MR data set, the automated segmentation of the proximal femur performed very well in the antero-superior and anterior femoral head-neck region with 95% HD values below 0.67 mm within these specific areas of clinical interest for cam-type morphology (see Fig 2).

### Cam Morphology in PT Patients

Within the PT male and female patients, there were no significant differences between baseline and 12-month cam volume, surface area, maximum height, or average height. This suggests that the PT protocol in the FASHIoN study did not alter cam bone mass (i.e., no bone “reduction”) in this specific cohort of patients

presenting with baseline mild, moderate, or major cam volumes. The lack of change in cam bone mass was well visualized in baseline and 12-month 3D models of the proximal femur in individual PT patients with very consistent regional topological and morphological characteristics of cam formations evident in the femoral head-neck ROI of these patients with FAI.

### Cam Morphology in AS Patients

The cam volume, surface area, maximum-height and average-height were significantly smaller for the 12-month compared to the baseline (preoperative) MR measures within both the AS managed male and female patients. In the present analyses, we had no specific information regarding the intended outcomes for bone resection in any of the AS-managed patients, limiting the ability to fully evaluate individual patient data. However, the median cam bone removal for the male

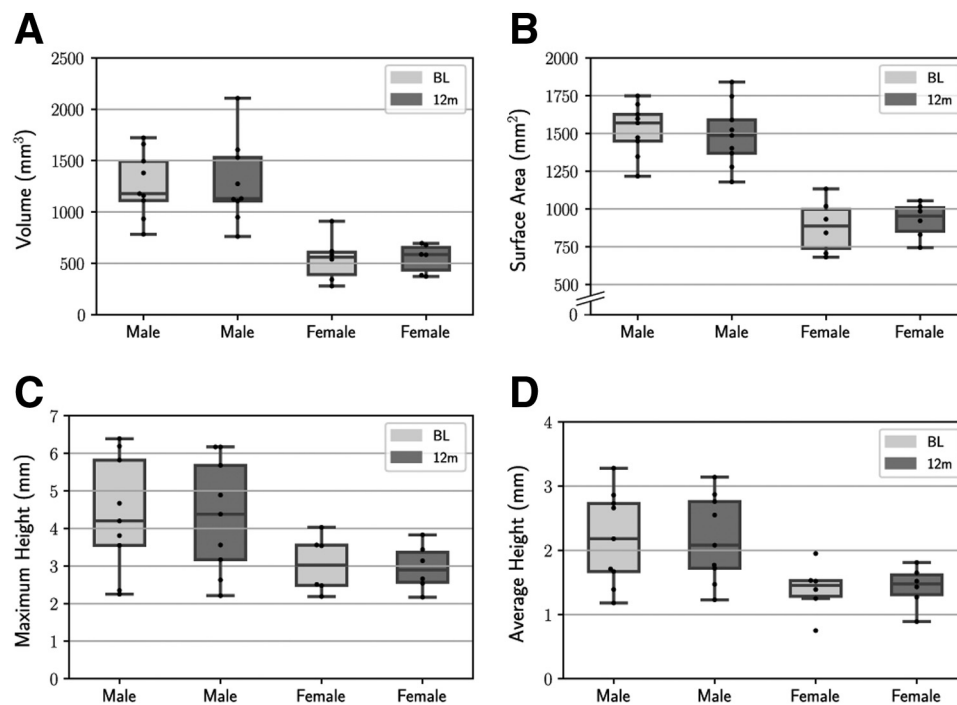


**Fig 3.** Boxplots for baseline and 12-month cam volume (A), surface area (B), maximum-height and (C) average-height (D) for male (*n* = 9) and female (*n* = 6) PT patients. The boxplot centerline marks the median value. BL, baseline; PT: physiotherapy; 12m, 12-months.

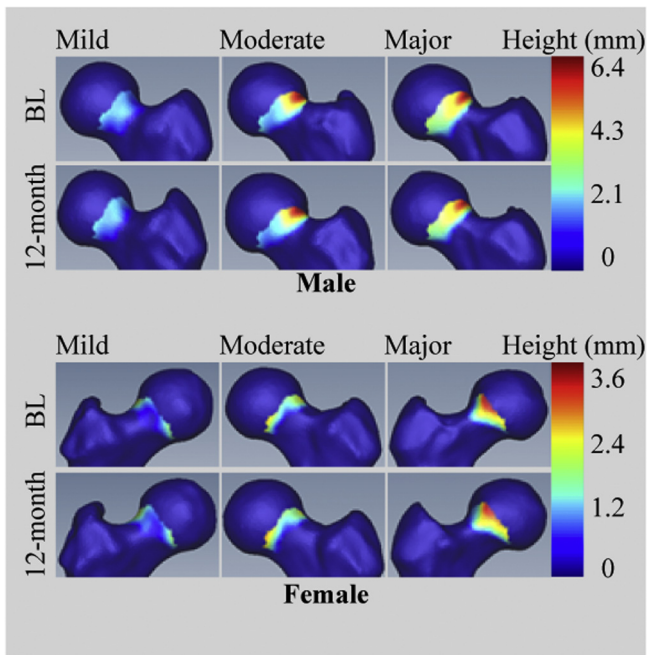


**Fig 4.** Visualization of 3D proximal femoral bone models at baseline and 12 months in individual male (rows 1 and 2) and female (rows 3 and 4) PT patients. The cases displayed include individual patients with a baseline mild (column 1), moderate (column 2), or major (column 3) cam volume. The dynamic range of the scalar bars for cam morphology height (in mm) was adapted for the different data range in male and female patients. BL, baseline; PT, physiotherapy.

and female AS patients for bone volume ( $653.5 \text{ mm}^3$ ,  $151.0 \text{ mm}^3$ ) and surface area ( $330.3 \text{ mm}^2$  and  $252.4 \text{ mm}^2$ ) were in good general agreement with the mean cam bone volume of  $939.9 \text{ mm}^3$  and surface area of  $615.8 \text{ mm}^2$  excised in arthroscopic surgeries performed on the hemipelvis of 7 cadavers (sex not specified) and analyzed with semiautomated segmentation from MR images.<sup>21</sup> Our median values for the resected cam bone for the male and female AS patients in terms of maximum height (0.81 mm, 0.58 mm) and average height (0.72 mm, 0.44 mm) were somewhat lower than the mean values in the cadaveric study of Guidetti et al.<sup>21</sup> (i.e., maximum height: 3.7 mm, average height: 1.6 mm). This may be attributable to a more

conservative “resection safety depth” in the AS patients related to concerns regarding over-resection of bone and unsafe thinning (weakening) of the femoral neck.

Reduced cam bone mass in the 12-month MR data in individual AS patients was well visualized in the anterior and antero-superior femoral head-neck junction, as shown in 3D models of the proximal femur. As per Fig 6, cam bone removal tended to be greater in the anterior and antero-superior femoral head-neck region compared to the antero-inferior region. However, it should be noted that when viewing the 3D bone models, we had no specific information regarding the intended outcomes for cam bone removal for individual patients, so the present observations are made without a priori knowledge on the amount or sites of bone/s identified for arthroscopic removal. Further, the data derived from the automated CamMorph pipeline, which was developed after the data collection in the Australian FASHIoN study,<sup>5</sup> were not obtained in the context of any planned preintervention (e.g., stratified allocation of patients to management arms) or postintervention purposes (e.g., evaluation of the location and amount of cam bone mass removal during ostectomy), nor with any a priori information regarding the (possible) location or size of cam formations in the FAI patients. The data generated by the automated CamMorph pipeline relate specifically to the cam morphology (volume, surface area, and height data) and location characteristics, as segmented from the baseline and 12-month MR images obtained from the male and female AS patients.

### Limitations

This study is not without limitations. In the present study, automated measurements of cam morphology were obtained from MR images using the 3D trueFISP sequence employed for structural hip imaging in the Australian FASHIoN study. Currently, the CamMorph pipeline has not been applied to other 3D MR sequences, such as VIBE and SPACE, previously shown to provide bone volumes comparable to CT in the knee joints of cadavers<sup>22</sup> or combined with functional MR imaging, such as dGEMRIC<sup>23</sup> and T2 mapping,<sup>24</sup> reported to be reliable in assessing hip cartilage integrity and degeneration.<sup>25,26</sup>

**Table 2.** Mean and Standard Deviation Data for Baseline and 12-Month Cam Volume, Surface Area, Maximum-Height and Average-Height in the Male and Female AS Patients

	Male ( $n = 18$ )		Female ( $n = 10$ )	
	Baseline	12-Month	Baseline	12-Month
Volume ( $\text{mm}^3$ )	$1342.73 \pm 678.87$	$718.08 \pm 552.91$	$498.93 \pm 325.57$	$240.24 \pm 186.58$
Surface area ( $\text{mm}^2$ )	$1520.32 \pm 253.19$	$1030.62 \pm 457.30$	$781.81 \pm 327.82$	$482.97 \pm 268.39$
Maximum height (mm)	$4.30 \pm 1.65$	$3.42 \pm 1.47$	$2.85 \pm 1.19$	$2.24 \pm 1.11$
Average height (mm)	$2.17 \pm 0.95$	$1.52 \pm 0.75$	$1.40 \pm 0.66$	$0.94 \pm 0.58$

AS, arthroscopic surgery.

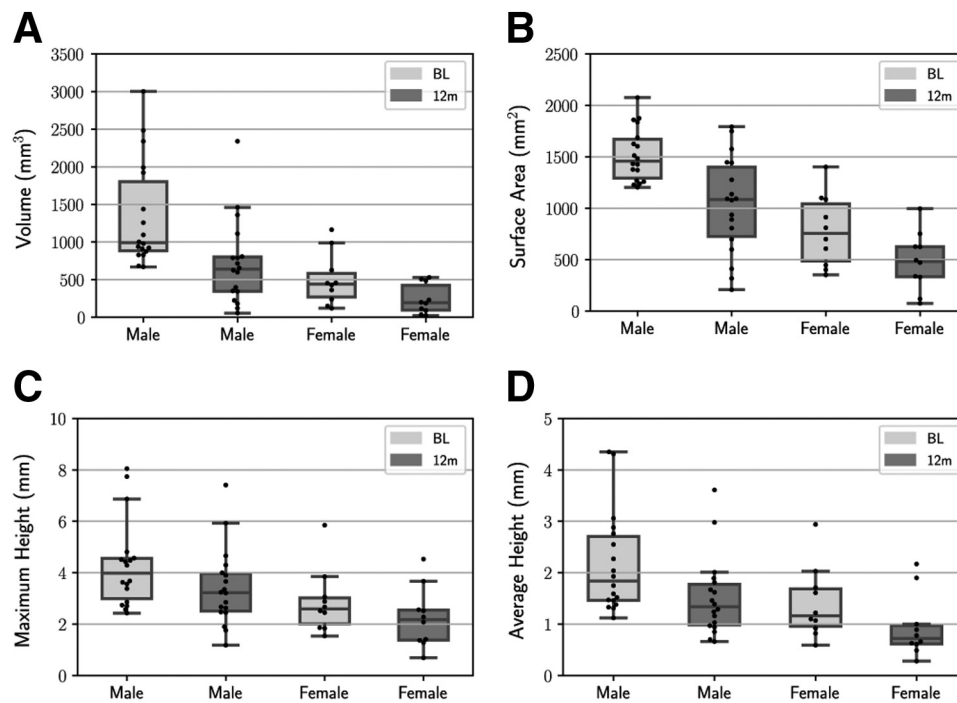


**Fig 5.** Boxplots for baseline and 12-month cam volume (A), surface area (B), maximum height (C), and average height (D) for male ( $n = 18$ ) and female ( $n = 10$ ) AS patients. The boxplot centreline marks the median value. AS, arthroscopic surgery; BL, baseline; 12m: 12-months.

Although the present work successfully implemented the 3D CamMorph pipeline for the automated measurement of cam morphology in the femoral head-neck region of FAI patients, currently an automated approach for measurement of pincer morphology has not been developed for the pipeline. Therefore, future work is needed to generate automated data on both pincer and cam morphology, as these osseous formations, either in isolation or combined in a “mixed” FAI presentation, are commonly evaluated for clinical decision making in patients with symptomatic FAI.<sup>1</sup>

Analysis of cam morphology in the 3D models of the proximal femur generated for the individual male and female FAI patients in the present study was limited to qualitative visualizations rather than quantitative shape analyses of cam location and topology. Potentially, quantifying cam shape characteristics in combination

with both cam and pincer morphology data has the potential for incorporation into personalized biomechanical models of the hip using techniques such as finite and discrete element modelling<sup>27,28</sup> to augment preintervention and postintervention evaluations in patients.

## Conclusions

Automated measurement of cam morphology from baseline (preintervention) and 12-month MR images demonstrated that the cam volume, surface area, maximum height, and average height were significantly smaller in AS patients following ostectomy, whereas there were no significant differences in these cam measures in PT patients from the Australian FASHIoN study.

**Table 3.** Median and Interquartile Range Data for Resected Cam Volume, Surface Area, Maximum-Height and Average-Height in the Male and Female AS Patients

	Male ( $n = 18$ )		Female ( $n = 10$ )	
	Median	Interquartile Range	Median	Interquartile Range
Volume ( $\text{mm}^3$ )	653.5	399.3 to 768.1	151.0	101.4 to 387.6
Surface area ( $\text{mm}^2$ )	330.3	266.2 to 615.9	252.4	132.3 to 321.5
Maximum height (mm)	0.81	0.38 to 1.59	0.58	0.39 to 0.99
Average height (mm)	0.72	0.42 to 0.90	0.44	0.24 to 0.69

AS, arthroscopic surgery.



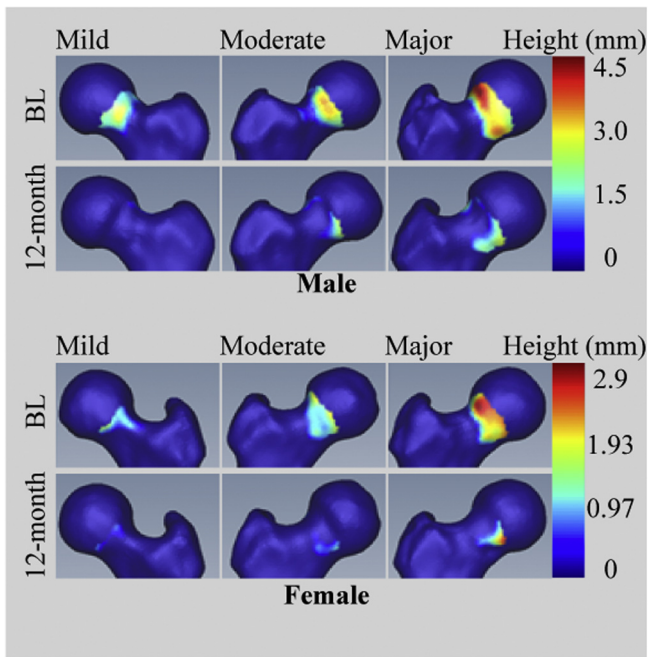


**Fig 6.** Visualization of three-dimensional proximal femoral bone models in individual male (rows 1 and 2) and female (rows 3 and 4) AS patients. The cases displayed include patients with baseline mild (column 1), moderate (column 2), and major (column 3) cam morphology. The dynamic range of the scalar bars for cam morphology height (in mm) was adapted for the different data range in male and female patients. AS, arthroscopic; BL, baseline.

### Acknowledgments

This work was supported by the University of Queensland and the Australian E-Health Research Centre under the Multi-Institutional Agreement for the National Health and Medical Research Council Development Grant APP1139868 entitled “MR Hip Intervention and Planning System to Enhance Clinical and Surgical Outcomes”.

### References

1. Griffin DR, Dickenson EJ, O'Donnell J, et al. The Warwick Agreement on femoroacetabular impingement syndrome (FAI syndrome): An international consensus statement. *Brit J Sports Med* 2016;50:1169-1176.
2. Sankar WN, Nevitt M, Parvizi J, Felson DT, Agricola R, Leunig M. Femoroacetabular impingement: Defining the condition and its role in the pathophysiology of osteoarthritis. *J Am Acad Orthop Surg* 2013;21:S7-S15 (Suppl 1).
3. Trigg SD, Schroeder JD, Hulsopple C. Femoroacetabular impingement syndrome. *Current Sports Med Rep* 2020;19:360-366.
4. Bugeja JM, Xia Y, Chandra SS, et al. Automated volumetric and statistical shape assessment of cam-type morphology of the femoral head-neck region from 3D magnetic resonance images (Preprint). *arXiv* 2021: 211202723.
5. Murphy NJ, Eyles J, Bennell KL, et al. Protocol for a multi-centre randomised controlled trial comparing arthroscopic hip surgery to physiotherapy-led care for femoroacetabular impingement (FAI): The Australian FASHIoN trial. *BMC Musculoskel Disord* 2017;18:406.
6. Yanke AB, Khair MM, Stanley R, et al. Sex differences in patients with CAM deformities with femoroacetabular impingement: 3-Dimensional computed tomographic quantification. *Arthroscopy* 2015;31:2301-2306.
7. Zhang L, Wells JE, Dessouky R, et al. 3D CT segmentation of CAM type femoroacetabular impingement –reliability and relationship of CAM lesion with anthropomorphic features. *Br J Radiol.* 2018;91:20180371.
8. Zilkens C, Tiderius CJ, Krauspe R, Bittersohl B. Current knowledge and importance of dGEMRIC techniques in diagnosis of hip joint diseases. *Skel Radiol* 2015;44:1073-1083.
9. Dice LR. Measures of the amount of ecologic association between species. *Ecology* 1945;26:297-302.
10. Litjens G, Toth R, van de Ven W, et al. Evaluation of prostate segmentation algorithms for MRI: The PROM-ISE12 challenge. *Med Image Anal* 2014;18:359-373.
11. Taha AA, Hanbury A. Metrics for evaluating 3D medical image segmentation: Analysis, selection, and tool. *BMC Med Imag* 2015;15:29.
12. Schroeder W, Martin K, Lorensen B. *The visualization toolkit*, 4th ed. New York, NY: Kitware, 2006.
13. Xia Y, Fripp J, Chandra SS, Walker D, Crozier S, Engstrom C. Automated 3D quantitative assessment and measurement of alpha angles from the femoral head-neck junction using mr imaging. *Physics Med Biol* 2015;60:7601-7616.
14. Virtanen P, Gommers R, Oliphant TE, et al. SciPy 1.0: Fundamental algorithms for scientific computing in Python. *Nature Methods* 2020;17:261-272.
15. Chandra SS, Dowling JA, Engstrom C, et al. A lightweight rapid application development framework for biomedical image analysis. *Computer Methods Prog Biomed* 2018;164:193-205.
16. Zeng G, Wang Q, Lerch T, et al. Latent3DU-net: Multi-level latent shape space constrained 3D U-net for automatic segmentation of the proximal femur from radial MRI of the hip In: *Paper presented at Machine Learning in Medical Imaging*. Copenhagen, Denmark: Cham, 2018.
17. Zeng G, Zheng G. Deep learning-based automatic segmentation of the proximal femur from MR images. In: Zheng G, Tian W, Zhuang X, eds. *Intelligent orthopaedics: Artificial intelligence and smart image-guided technology for orthopaedics*. Singapore: Springer Singapore, 2018;73-79.
18. Peng B, Guo Z, Zhu X, Ikeda S, Tsunoda S. Semantic segmentation of femur bone from MRI images of patients with hematologic malignancies In: *Paper presented at 2020 IEEE Region 10 Conference (Tencon)*, Osaka, Japan; Nov 16-19 2020.
19. Memiş A, Varlı S, Bilgili F. Semantic segmentation of the multiforum proximal femur and femoral head bones with the deep convolutional neural networks in low quality MRI sections acquired in different MRI protocols. *Comput Med Imag Graphics* 2020;81:101715.
20. Deniz CM, Xiang S, Hallyburton RS, et al. Segmentation of the proximal femur from MR images using deep convolutional neural networks. *Scientif Rep* 2018;8:16485.

21. Guidetti M, Malloy P, Alter TD, et al. MRI-and CT-based metrics for the quantification of arthroscopic bone resections in femoroacetabular impingement syndrome. *J Orthop Res* 2022;40:1174-1181.
22. Neubert A, Wilson KJ, Engstrom C, et al. Comparison of 3D bone models of the knee joint derived from CT and 3T MR imaging. *Eur J Radiol* 2017;93:178-184.
23. Hunter DJ, Eyles J, Murphy NJ, et al. Multi-centre randomised controlled trial comparing arthroscopic hip surgery to physiotherapist-led care for femoroacetabular impingement (FAI) syndrome on hip cartilage metabolism: The Australian FASHIoN trial. *BMC Musculoskel Disord* 2021;22:697.
24. Ho CP, Surowiec RK, Frisbie DD, et al. Prospective in vivo comparison of damaged and healthy-appearing articular cartilage specimens in patients with femoroacetabular impingement: Comparison of T2 mapping, histologic endpoints, and arthroscopic grading. *Arthroscopy* 2016;32:1601-1611.
25. Mamisch TC, Kain MSH, Bittersohl B, et al. Delayed gadolinium-enhanced magnetic resonance imaging of cartilage (dGEMRIC) in femoacetabular impingement. *J Orthop Res* 2011;29:1305-1311.
26. Wyatt C, Kumar D, Subburaj K, et al. Cartilage T1ρ and T2 relaxation times in patients with mild-to-moderate radiographic hip osteoarthritis. *Arthritis Rheumatol* 2015;67:1548-1556.
27. Ateshian GA, Henak CR, Weiss JA. Toward patient-specific articular contact mechanics. *J Biomech* 2015;48:779-786.
28. Li M, Venäläinen MS, Chandra SS, et al. Discrete element and finite element methods provide similar estimations for hip joint contact mechanics during walking gait. *J Biomech* 2021;115:110163.